Journal of Heat and Mass Transfer Research

Journal homepage: http://jhmtr.semnan.ac.ir

Semnan University

Chilled Ceiling Effects on The Indoor Air Quality in a Room Equipped with Displacement Ventilation System

Sarvenaz Arzani[a], Bahram Rahmati[b], Amir Mohammad Jadidi [*,b]

[a]*Faculty of Mechanical Engineering, Concordia University, Montreal, Canada.*
[b]*Faculty of Mechanical Engineering, Semnan University, Semnan, Iran.*

PAPER INFO

Paper history:
Received: 2021-03-15
Revised: 2021-07-23
Accepted: 2021-08-09

Keywords:
Air Quality (IAQ);
Chilled ceiling (CC);
Displacement ventilation (DV);
Local exhaust vent (LEV).

ABSTRACT

Over time, many studies have proven the advantages of using chilled ceiling systems as an assistant device for covering the barriers of the stratified air distribution systems. However, previous investigations are still insufficient, especially in analyzing indoor air quality. With the aid of the computational fluid dynamics techniques and Airpak software, we attempted to determine the possible effects of the chilled ceiling on the performance of displacement ventilation by evaluating contaminant removal, ventilation effectiveness, the freshness of air, and air change efficiency. In addition, we tried to find a solution to maintain the stratified form of the contaminant profile, and reduce the impact of the negative buoyant flow caused by the chilled surface. In order to investigate, the study was analyzed with variable exhaust vent location. The results indicated that the indoor air quality indexes had the best operation compared to the other cases when the exhaust vent was placed near the occupants. Actually, by local exhaust vent strategy, the inversion phenomenon caused by chilled surface was minimized and the contaminant concentration was safer at the inhaled zone compared to the other cases. In addition, the chilled ceiling had entirely adverse effects on the mean age of air, contaminant concentration, air change efficiency and ventilation effectiveness. Nevertheless, the disturbance effect was lower when the exhaust vent placed in the vicinity of heat/contaminant sources.

DOI: 10.22075/JHMTR.2021.22921.1337

© 2021 Published by Semnan University Press. All rights reserved.

1. Introduction

Nowadays, heating, ventilating, and air-conditioning (HVAC) systems are considered as the heart of the buildings. The chilled ceiling (CC) or radiant cooling systems have gained popularity in residuals and non-residual buildings, particularly in Asia and Europe [1,2] due to the positive effects on thermal comfort, vertical gradient temperature, and indoor air quality [3,4]. Researches on the CC systems have been started since the 1990s [5]. Usually, the design of the CC panels is expanded into three categories. Embedded tubes inside the concrete slab of buildings are the most common design of the chilled panels [6]. Despite the advantages, the CC systems have two issues. Firstly, the low temperature of the water inside the tubes causes the risk of condensation on the CC panels [7,8]. Secondly, the system couldn't remove the latent loads, and renew the indoor air. Therefore, these systems need to be coupled with an air distribution system to fulfill the ventilation standards and be able to eliminate the latent loads and the indoor pollutants [9,10].

In recent decades, the stratified air distribution (STRAD) systems, may be referred to as under-floor distribution (UFAD) or displacement ventilation (DV) systems, have gained the attention of people who are willing to have an optimized indoor air quality (IAQ) and thermal comfort (ITC) [11,12]. In these systems, the inlet air diffusers are located on the floor which the temperature and the contaminant profiles are completely stratified [11]. Some researchers concluded that CC systems could provide cooler environments compared to traditional systems [13,14]. Miriel et al. [15] reported that the CC system was suited for buildings with low-cooling loads. They reported that the temperature of panels should be limited in case of condensation. This subject drops the cooling capacity. Therefore, to avoid condensation, the temperature of the panels should be under the dew point of a room in the subtropical region [16].

[*]*Corresponding Author: Amir Mohammad Jadidi, Faculty of Mechanical Engineering, Semnan University, Semnan, Iran.*
Email: am.jadidi@semnan.ac.ir

In numerous studies, CC systems with displacement ventilation (DV) have been suggested since the hybrid system has increased the cooling capacity and has provided higher air quality and thermal comfort indexes [17,18]. Loveday et al. [19] reported that the cooled air under the DV-CC system could cause a downward convection flow, which transports the contaminant to the inhaled zone. Ghaddar et al. [20] investigated a design algorithm for a DV-CC system. The study was based on four parameters:

(1) The ratio of the chilled ceiling cooling load to the total load, (2) The vertical temperature profile, (3) IAQ, (4) the ratio of the total sensible load to the supply air mass flow rate. By investigating these factors, the design charts were displayed for a steady-state flow for a wide range of chilled ceiling tempearures and supply air. Xie et al. [21] investigated the impact of the inlet water temperature on the non-uniform surface temperature of the chilled panel. The radiant ceiling panel with a uniform temperature distribution was studied by Ning et al. [22] to prevent condensation. Furthermore, Behne [23] suggested that DV should remove 20 to 25% of the heat loads for a suitable IAQ and ITC in a DV-CC system.

On the other hand, DV or UFAD systems have a supply plenum between the concrete slab and a raised floor system to push fresh air directly into the occupied zone through floor diffusers. UFAD (or DV) systems have some beneficiaries like: suitable thermal stratification, thermal comfort, ventilation efficiency, and reduced energy use in suitable climates [24]. These advantages make it a good candidate in order to integrate with chilled ceiling system. As it was mentioned in some previous studies, there are numerous researches in different combinations of radiant cooling with displacement ventilation, but there are a few types of research about the integrated UFAD-Radiant system in the literature. Performance analysis of an integrated UFAD and radiant hydronic slab system has been done by Raftery et al. [25]. They used EnergyPlus and their study to prove that the UFAD-Radiant system reduces 23% of total energy consumption rather than overhead systems. Also, the thermal comfort of occupant improved, and some thermal decays of UFAD were extinguished.

The recent studies on CC/DV systems are insufficient, especially on IAQ study. In this article, we combined the CC with the DV system to clarify the effects of chilled surface on IAQ in a room equipped with DV system. More importantly, we tried to find a solution to reduce the disturbance effect of the chilled surface on the contaminant distribution. As the exhaust vent has a critical role in airflow formation, several places for exhaust vent were considered case studies. The considered positions for the exhaust vent included ceiling exhaust vent (CEV), low height exhaust, and local exhaust vent (LEV) strategy.

CEV strategy is a common way for the exhaust vent, and all of the mentioned investigations were conducted with this strategy. On the other hand, with LEV strategy, it is possible to transfer the contaminant and heat loads immediately out of the occupied zone due to the small distance with the exhaust vent. LEV is not a method of ventilation. It is used for controlling pollutants, especially in industrial, aircraft cabins, and hospital environments with high efficiency. LEV strategy provides a good potential for hybrid systems in which use chilled surfaces. That is because the contaminant can exit from the occupied zone by LEV before any interaction with the negative buoyant flow at the ceiling.

The disadvantage of the CC to exhaust pollutant from breathing zone has been addressed by Yang et al [26], and Shi et al. [27]. To overcome these cons, the combination of the chiled ceiling with the displacement ventilation and the under-floor air distribution is recommended. In this study, we tried to use an assistant (LEV) to take pollutant particles into exhaust vents as an aid to the CC. In another word, by this kind of hybridization the CC acts as a background system and the LEV is used to prevent pollutants from aggregation in the inhaled zone. It should be noted that combination of the CC and the LEV is not explored yet. IAQ indexes including ventilation effectiveness and normalized concentration are investigated to depict the importance of the hybridization of CC and LEV.

2. Methods

2.1. Airflow Modeling

In order to simulate a CC/DV system in a room, computational fluid dynamics (CFD) was applied to predict indoor air. The commercial CFD program Airpak 3.0.16 was used for designing the geometry and solving the Reynolds averaged Navier-Stokes (RANS) equations. The following assumptions were employed for calculation:

- 3D turbulent flow
- Steady-state
- Incompressible fluid flow

The Governing equations were as follows:

Continuity equation:

$$\nabla \cdot \vec{v} = 0 \tag{1}$$

Where $\vec{v}$ is the air velocity.

Momentum equation:

$$\nabla \cdot (\rho \vec{v} \vec{v}) = -\nabla P + \nabla \cdot (\bar{\bar{\tau}}) + \rho \vec{g} \tag{2}$$

Where ρ is obtained from the ideal gas equation $\rho = \frac{P_{op}}{\frac{R}{M_w}T}$. In the ideal gas law equation, $P_{op}$is the operating pressure, R is the universal gas constant and M_w is the molecular weight of the gas. Also, P is the static pressure of air, $\rho \vec{g}$ is the gravitational body force, and $\bar{\bar{\tau}}$ is the stress tensor, calculated using the equation $\bar{\bar{\tau}} = \mu[(\nabla \vec{v} + \nabla \vec{v}^T)]$. In the stress tensor equation, μ is the molecular viscosity, and I is the unit tensor.

Energy conservation equation:

$$\nabla \cdot (\rho h \vec{v}) = \nabla \cdot [(k + k_t)\nabla T] + S_h \quad (3)$$

Where h is the sensible enthalpy, obtained from the equation $h=\int_{T_{ref}}^{T} C_p dT$ where $T_{ref} = 298.15\ K$, k is the molecular conductivity, k_t is the conductivity due to turbulent transport, which is calculated using the equation $k_t=\frac{C_p \mu_t}{Pr_t}$, S_h is the source term which includes all defined volumetric heat sources

Species transport equation:

$$\nabla \cdot (\rho \vec{u} Y_i) = -\nabla \cdot \vec{J}_i + S_i \quad (4)$$

Where, Y_i is the local mass fraction of each species, S_i is the rate of creation by addition from defined sources and $\vec{J}_i$ is the diffusion flux of species and is calculated from the equation $\vec{J}_i = -(\rho D_{i.m} + \frac{\mu_t}{Sc_t})\nabla Y_i$. In the diffusion flux of species equation, $D_{i,m}$ is the mass diffusion of each species, μ_t is the turbulent viscosity and Sc_t is the turbulent Schmidt number (Sc_t = 0.7).

The indoor zero equation was used for calculation of the turbulent viscosity. Indoor zero equation turbulence model was introduced by Chen and Xu [28]. This model was successful in simulating of the indoor airflows based on the previous investigations and more importantly, it helped the HVAC engineers due to its simple way of calculation. Eq. (5) determines the details of the equation.

$$\mu_t = 0.03874\, \rho \cdot v \cdot l \quad (5)$$

Where l is the distance from the nearest wall and 0.03874 is an empirical constant.

The surface-to-surface radiation model was employed to simulate the effects of the radiation inside the chamber. The model is an economical and fast way to calculate the radiation effects in most applications. In order to introduce the pressure to the continuity equation, SIMPLE (Semi-Implicit Method for Pressure-Linked Equations) algorithm was used. All of the mentioned quantities were computed using the second-order upwind scheme approach for discretization.

2.2. Validation

Before simulation of the CC/DV system, we simulated the experimental investigation in which conducted by Kobayashi and Chen [29] only to show the amount of error in the numerical simulation. Fig. 1 shows the details of the validation case. The interior settings and wall boundary conditions are listed in Table 1. The main manuscript determined 9 poles throughout the room to show the temperature, velocity, and sulfur hexafluoride (SF_6) profiles. In order to achieve a close trend with the experimental data of temperature, velocity, and SF_6, several meshes were tested. According to the results, the number of 1782599 of three-dimensional hexahedral cells was adequate for a precious simulation. The mentioned cell numbers took approximately 5000 iterations for the governing equations to meet the convergence criteria (10^{-4}) for continuity equation. Fig. 2 shows the achieved profiles by simulation in comparison with the experimental data. Due to the main article preference, the temperature and SF_6 are presented dimensionless.

Table 1. The summary interior settings of the tested office

Air change per hour		4.4		
Supply temperature		19℃		
Walls boundary conditions	North	26.8℃	West	25.8℃
	South	26.8℃	Floor	25.0℃
	East	28.6℃	Ceiling	27.4℃
Internal heat sources	Lamps	4 × 68 W	PC-1	108.5 W
	Persons	2 × 75 W	PC-2	173.4 W
	Sum	703.9 W		

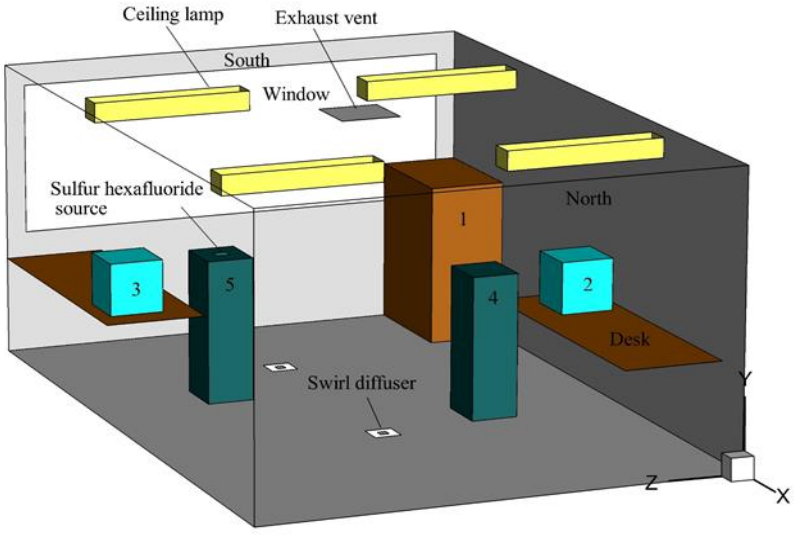

Fig. 1. Configuration of Kobayashi et al. [29] chamber; 1 – shelf 2 – PC-1 3 – PC-2 4 – Occupant 1 5 – Occupant 2.

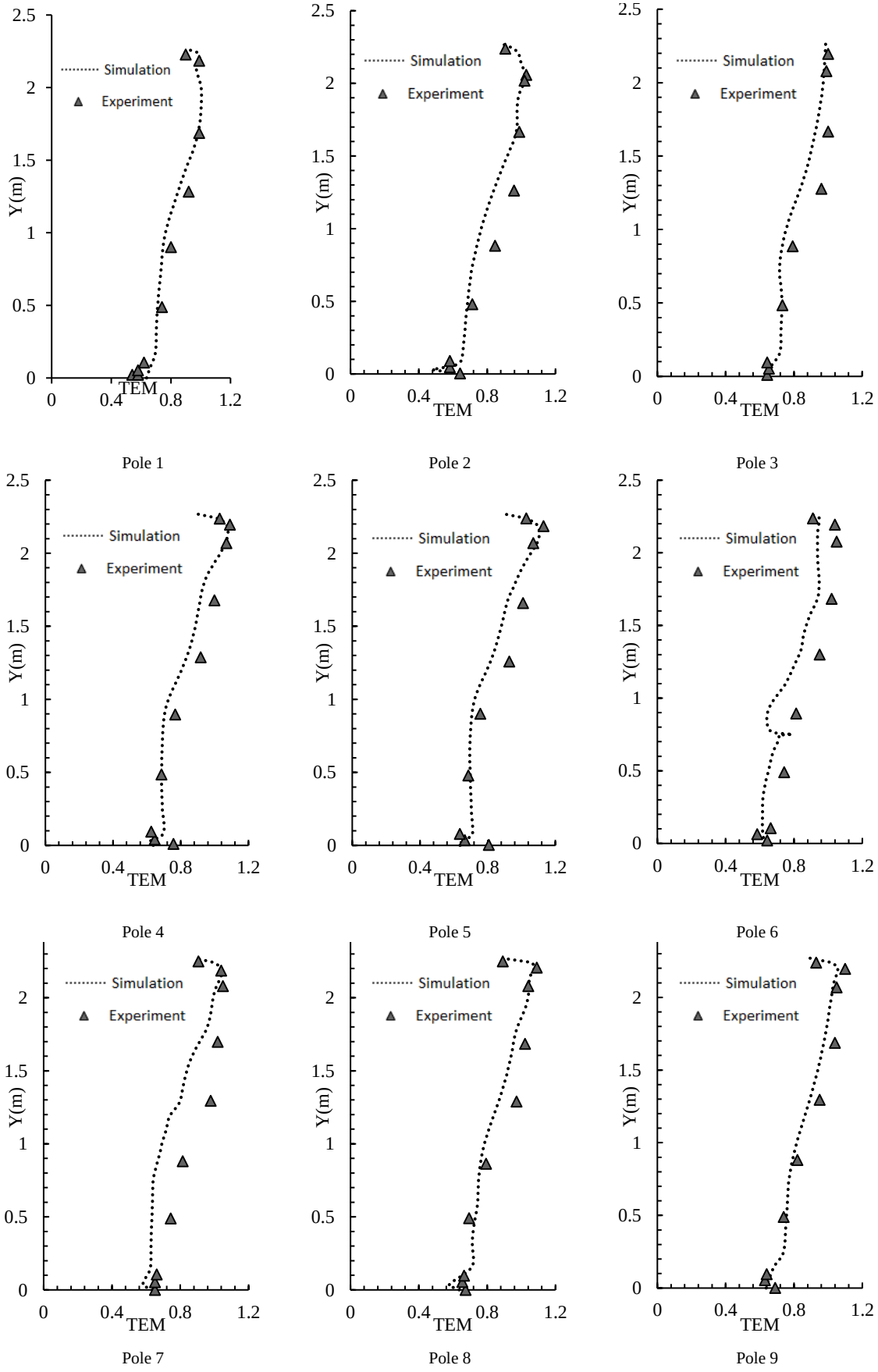

Fig. 2(a). comparison between numercial and experimental data of temperature profiles: TEM = $(T-T_{supply}) / (T_{exhaust}- T_{supply})$

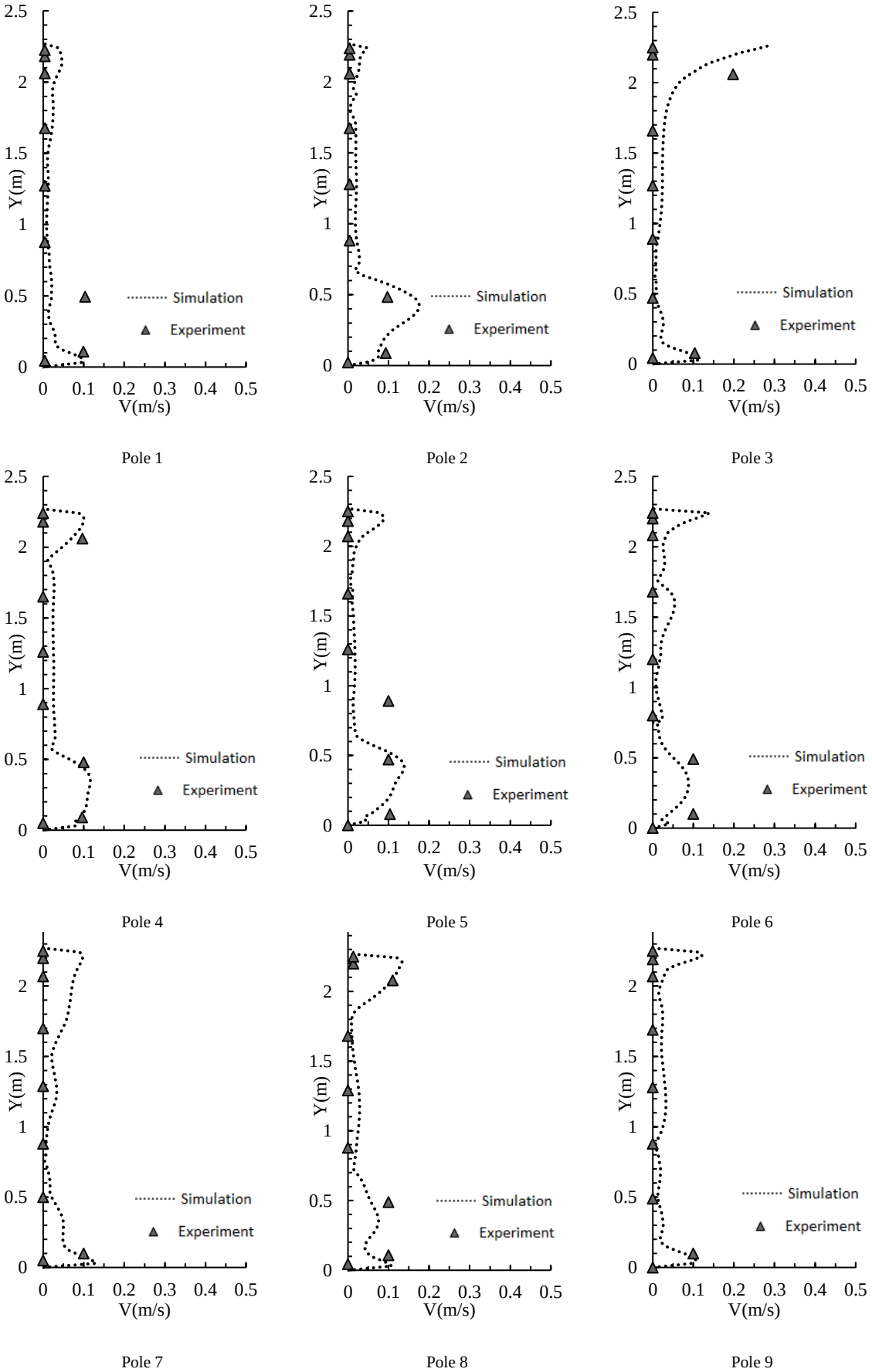

Fig. 2(b). comparison between numerical and experimental data of velocity profiles

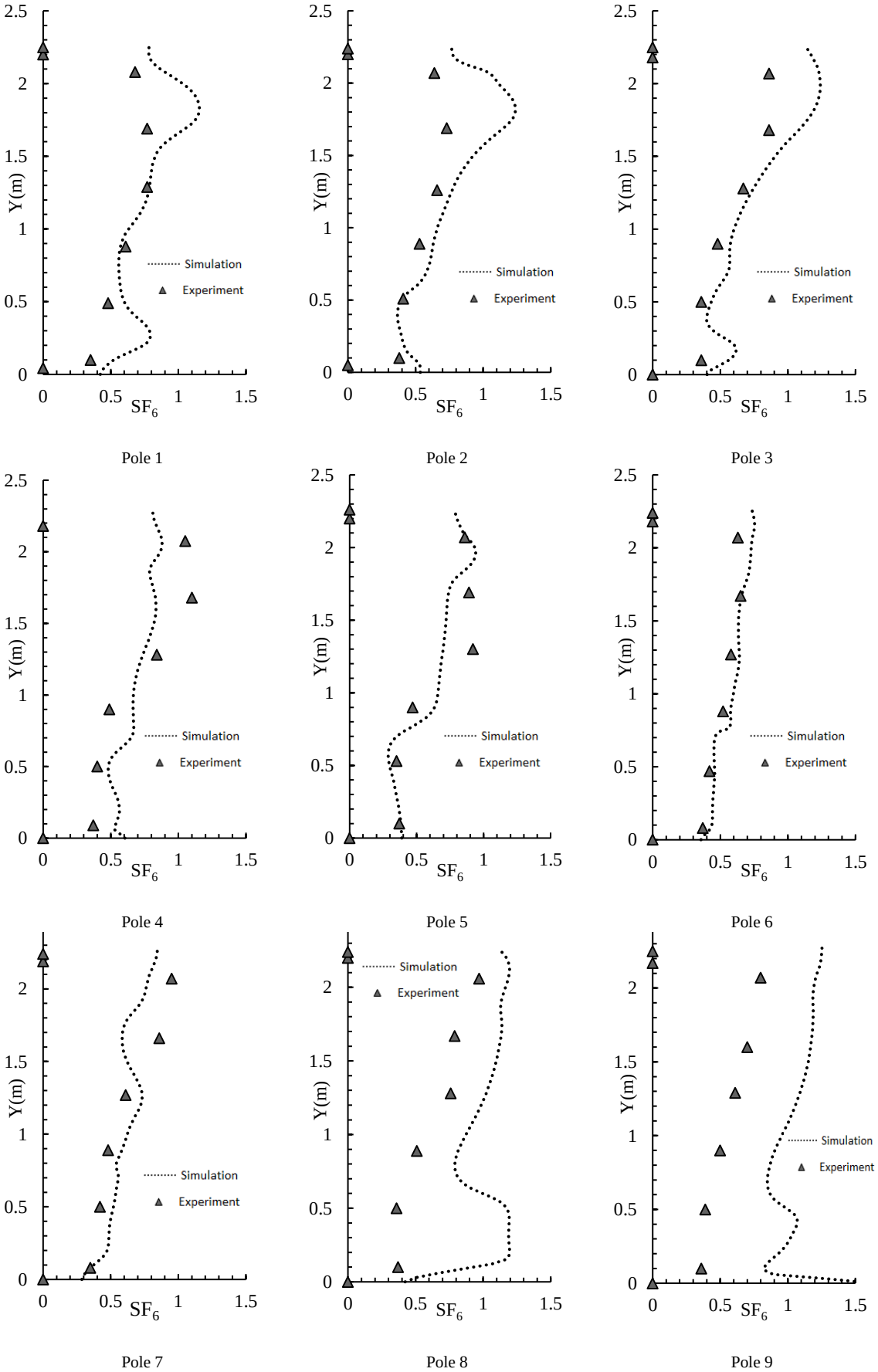

Fig. 2(c). comparison between numerical and experimental data of SF_6 concentration profiles:

$$SF_6 = (SF_6 - SF_{6\ inlet})/(SF_{6\ exhaust} - SF_{6inlet})$$

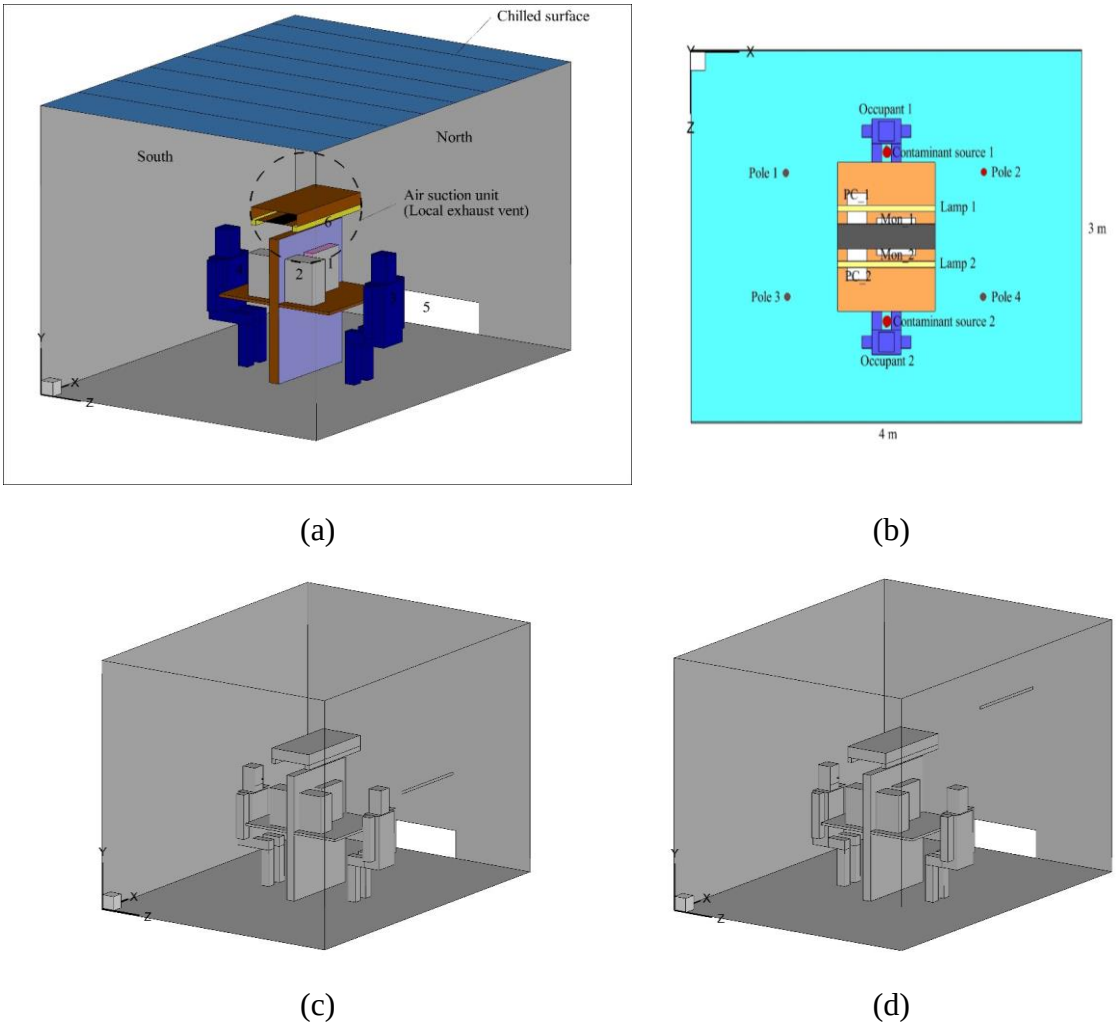

Fig. 3 (a) Configuration of the cases 1 and 2; 1 – PC monitor; 2 – PC case; 3 and 4 – Occupants; 5 – Lamps; 6 – Local exhaust vent; 7 – exhaust vent terminal; 8 – Displacement diffuser; (b) positions of poles, contaminant and heat sources; (c) case 3; (d) case 4.

The method to transfer the data to a non-dimensional form in these two fields is provided in figure captions of Fig. 2. According to the simulation results, the simulated trend agreed well with the experimental data in most of the poles (except some errors in poles 1 and 5 of velocity filed) of temperature and velocity filed (see Figs. 2a and 2b). Nevertheless, a great difference was occurred between our simulations and the experimental trend in SF_6 profile around the contaminant source (see Fig. 1c pole 8 and 9). According to the main manuscript, the tracer-gas source was a point source, and the contaminant was very sensitive to the position. Despite this problem, the other poles of the contaminant profile were well simulated compared to the experimental measurements. This result indicating that the numerical approach which was explained in the airflow modeling was reasonable.

2.3. Scenarios

Fig. 3 shows the simulated room of the target model. The size of the room was 4 m length, 3 m width and 2.7 m height. The simulated heat sources and the released heat from each of them are listed in Table 2. The total air volume and the supply temperature were 4 ACH (air change per hour) and 20°C, respectively. As mentioned, three exhaust vent locations were considered to investigate the effects of chilled ceiling on the IAQ.

Fig. 3 (a) shows cases 1 and 2. The difference of these cases was the position of the exhaust vent. In case 1 the exhaust vent was placed at the ceiling (The traditional location for the exhaust vent) and was combined with the chilled surface.

Table 2 the summary conditions of heat sources in the simulated office

Internal heat sources	Cooling load (W)
Occupants	70 × 2
PC-case	50 × 2
PC-monitor	65 × 2
Light-Simulator	24 × 2
Total	418

Case 2 represents the LEV strategy, which means the air suction unit was active. In this case, the polluted air leaves the micro-climate around the occupants via the air suction device. Case 3 represents low height exhaust vent strategy (see Fig. 3c). Generally, the exhaust vent must be located at high heights or even at the ceiling in the STRAD systems. However, in some cases, the low-height exhaust vent strategy improved the particle removal efficiency. Since the role of the chilled surface is still unknown in the contaminant removal of a system, it was reasonable to check the performance of the hybrid CC/DV in the low height of the exhaust vent.

Case 4 also shows another common place for the exhaust vent. Aside from comparison between cases, each case study was also compared with the base model of themselves (Without chilled ceiling) to find out the possible disturb or improvement effect of a chilled surface. Therefore, computation was solved with/without the chilled surface for each case study. As the design range for temperature of the chilled ceiling is between 16 to 19 ℃, the chilled surface temperature in this study was considered 17℃ for all of the hybrid case studies. The area of the chilled ceiling in the hybrid mode was the entire roof (see Fig. 3a). For the standalone cases (without chilled surface), the temperature of the ceiling was 27.4℃ which was the main boundary condition.

The contaminant sources of the geometry were the exhaled air of the occupants. Two opening units for CO_2 gas were placed at the height of the 1.1 m from the floor to simulate the occupants' nose. The direction of the opening diffusers was designed as 45° below horizontal axis. The temperature and speed of the occupants' exhaled air were equal to be 34℃ and 0.7 m/s, respectively. As the human exhaled air contains nitrogen, oxygen, carbon dioxide, and argon, carbon dioxide (CO_2) was selected to represent the distribution of the pollution inside the office. Therefore, the considered mass fraction for the CO_2 was equal to 5 percent, which is the real proportion of this gas rather than other contaminants in the human exhaled mixture. The considered boundary condition of the exhaust vent was pressure-outlet. As mentioned, the target model had no experimental data. Consequently, before computing the scenarios, we conducted the grid indecency test.

2.4. Grid study

The aim of this section is determination of the required number of cells in the target model. Since there were no massive geometrical changes in the scenarios, only one scenario was selected to perform the grid independency test. The selected case study was case 1 without chilled surface. In order to do the test, four numbers of cells were considered. Furthermore, in order to achieve high precision, all of the tested scenarios had more cells in the vicinity of the occupants, heat sources, inlets, and the outlet diffusers. The Considered number of cells are listed in Table 3. As it was mentioned, the grid study was conducted at the introduced poles of Fig. 1.

Table 3 The nodes number in grid study precedure

Grid type	Number of elements	Number of grid nodes
Mesh_1	123.212	134.014
Mesh_2	617.256	651.710
Mesh_3	1.252.725	1.300.259
Mesh_4	1.711.943	1.768.303

According to Fig. 4, there was no significant changes by increasing the cell numbers from mesh_2, mesh_3 and mesh_4 in the temperature and velocity field. However, the difference between Mesh_2 and Mesh_3 was found in the contaminant profile. Briefly, by considering all of the profiles, there was no significant change by increasing the cell numbers from Mesh_3 to Mesh_4. Therefore 1252725 elements were adequate for a precious simulation. Similar cell numbers were used for the other scenarios.

3. Evaluation indexes

3.1. Temperature distribution

The vertical temperature gradient is one of the vital factors for analyzing the occupant's indoor thermal comfort in a room. According to ISO7730 [30], if the temperature difference between head level (1.1m from the floor) and the feet level (0.1m from the floor) exceeds more than 3ºC, occupants may feel the local thermal discomfort. Moreover, ASHRAE Standard 55 [31], defined the favorable mean room air temperature between 23 to 26°C.

3.2. Indoor air quality (IAQ) criteria

The considered indexes for the post-processing phase of IAQ was normalized CO_2 concentration at the introduced poles and at the inhaled zone, ventilation effectiveness, mean age of air (MAA) and air change efficiency (ACE). All of the mentioned indexes are representing the air quality inside the office. Eq. (6) shows the normalized concentration:

$$\varepsilon_n = \frac{C - C_s}{C_e - C_s} = \frac{C}{C_e} \tag{6}$$

Where C is the pollution at a point or area somewhere in the space where (in this study is either concentration at the introduced poles or the inhaled zone), C_e is the pollution at the exhaust vent and C_s is the pollution at the opening diffuser (here $C_s = 0$). It is clear that the lower values of ε_n shows the healthier inhaled environment for the occupants. For diluting base systems like the traditional MV systems, ε_n is equal to unity. Values more than unity shows that the considered position for calculation has more contaminant compared to the concentration at the exhaust vent. Comparing to Eq. (6), ventilation effectiveness is defined as:

$$\varepsilon_e = \frac{C_e - C_s}{C_p - C_s} = \frac{C_e}{C_p} \tag{7}$$

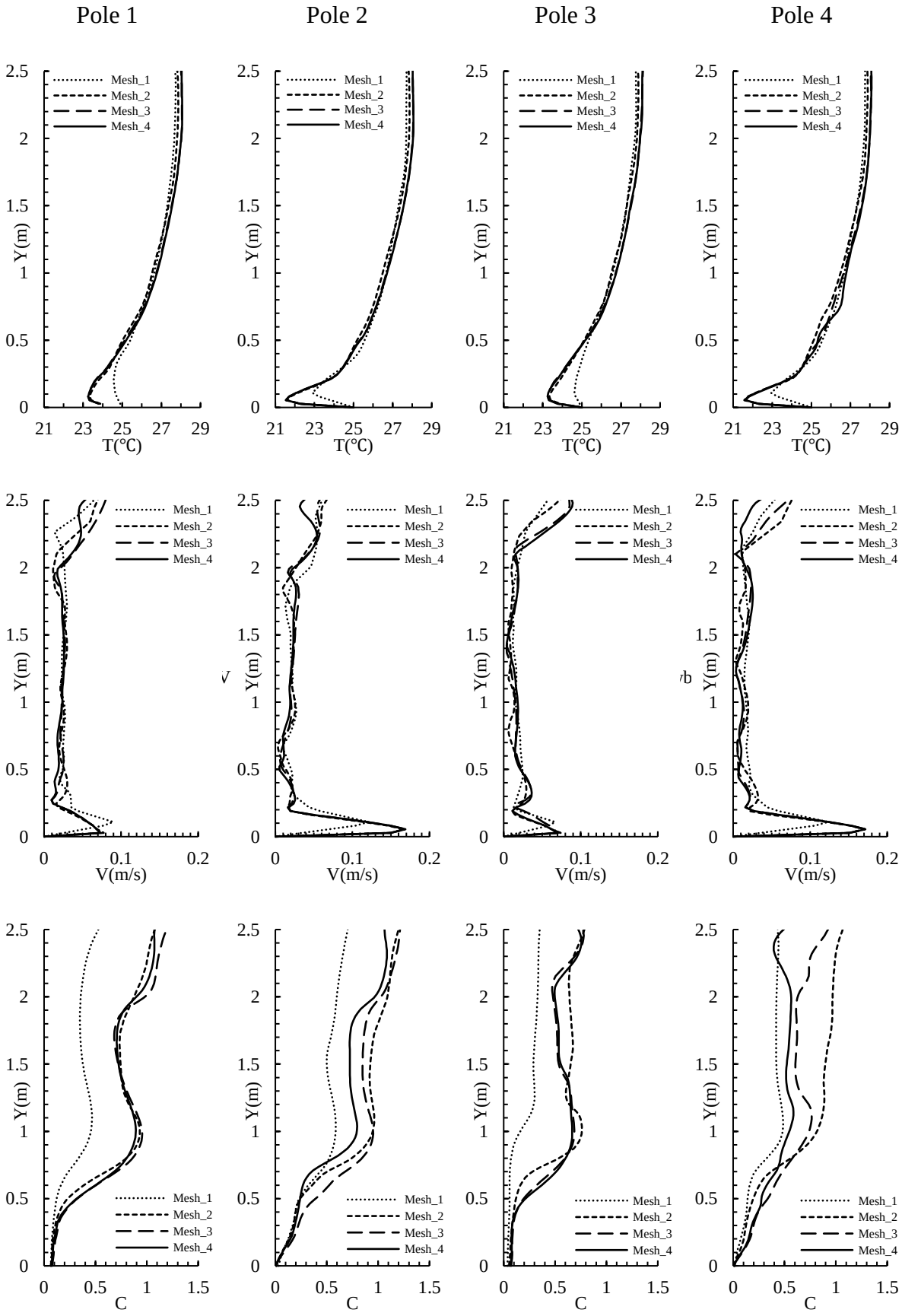

Fig. 4 Grid independency results

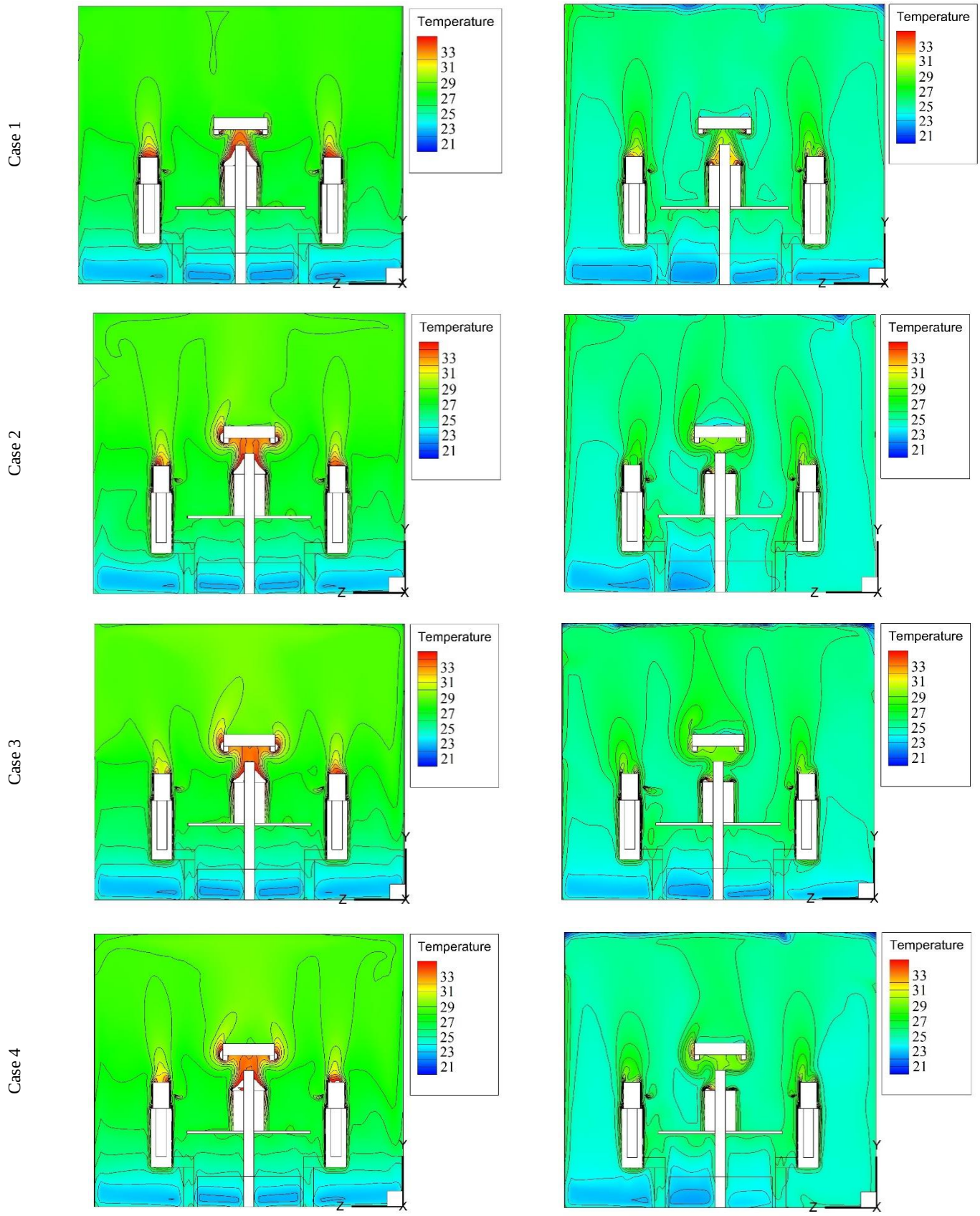

Fig. 5. Comparison of temperature (°C) contours between DV and Hybrid scenarios

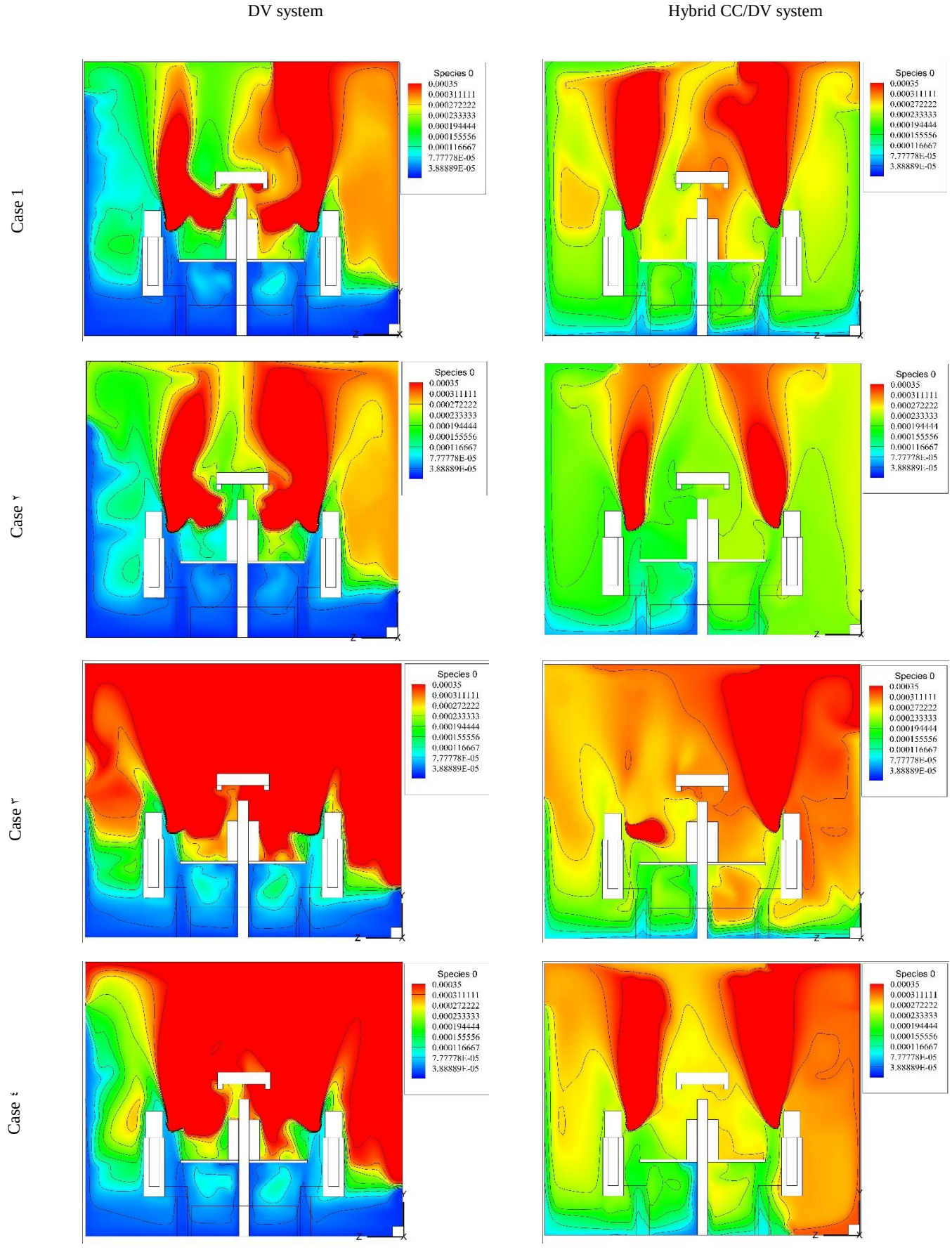

Fig. 6. Comparison of contaminant contours between DV and Hybrid scenarios

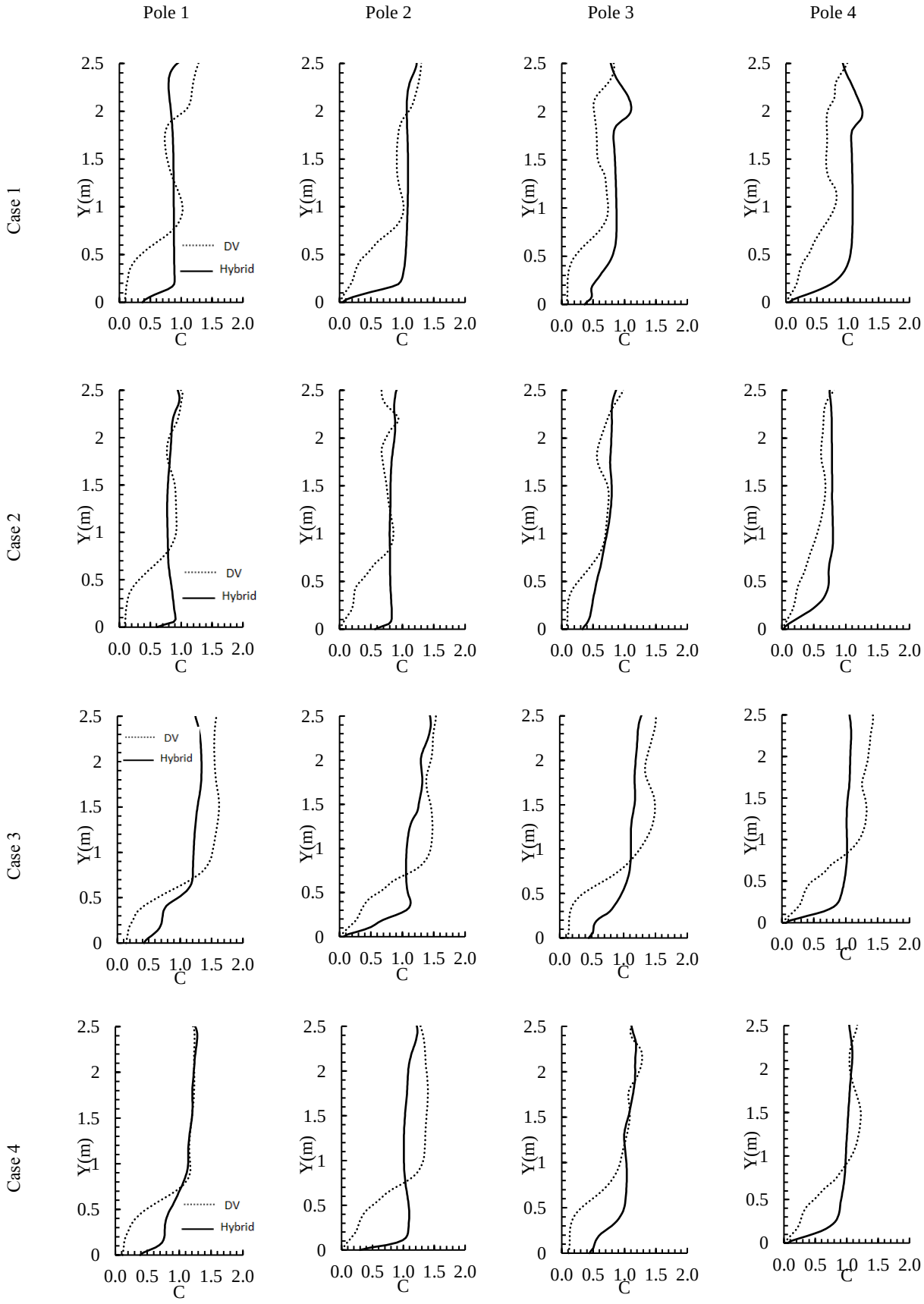

Fig. 7. Normalized contaminant distribution between DV (dash lines) and hybrid scenarios

Table 4. The results of temperature distribution analyze

Case study	Local thermal discomfort					
	Occupant 1		Occupant 2		Mean room temperature	
	DV	CC/DV	DV	CC/DV	DV	CC/DV
1	3.8	1.8	3.4	1.6	26.7	24.7
2	2.3	1.0	3.4	1.0	26.8	24.7
3	3.8	1.9	3.8	1.8	27.1	25.1
4	4.0	1.3	3.5	0.9	27.0	24.7

Where C_p is the mean concentration in the occupied zone (0-1.3 m from floor), C_e is the concentration at the exhaust vent. Contrary to the normalized concentration, the more values of ε_e represents the better ventilation scenario for the office. The acceptable value for a STRAD system is above 1.2 [31].

MAA index evaluates the freshness of the operating air. Actually, MAA is the average lifetime of air molecules at a certain position based on the time which they were entered the room. As it is clear, the older age of air represents the poorer air transference. The MAA is governed by the following transport equation:

$$\frac{\partial}{\partial t}(\rho\tau) + \frac{\partial}{\partial x_j}\left(\rho u_j \tau\right) = \frac{\partial}{\partial x_j}(\Gamma_t \frac{\partial \tau}{\partial x_j}) + \rho \qquad (8)$$

Where τ is the mean age of air (s), Γ_t is the effective diffusion coefficient (dimensionless) and ρ is the fluid density (kg/m^3). Also, $\tau = 0$ at the supply diffuser and $\frac{\partial \tau}{\partial x_j} = 0$ at the exhaust vent and the walls are boundary conditions. For calculating the MAA in breathing zone a cubature was assumed in front of each occupant at the height of 1.1 m from the floor.

ACE is an index for quantifying the ability of a system to renew the air in the room, and it is defined as the ratio between the minimum and the actual mean replacement times. The ACE was obtained from the following equation:

$$\varepsilon_a = \frac{V/Q_e}{2\bar{\tau}_a} \times 100 = \frac{\tau_n}{2\bar{\tau}_a} \times 100 \qquad (9)$$

Where V is the air volume of the enclosed space, Q_e is ventilation flow rate, and τ_n is the nominal time constant or the mean age of air in the exhaust which is equal to V/Q_e and $\bar{\tau}_a$ is the room mean age of the air. The ACE index is between 0 and 100%. For a stratified flow ε_a is between 50% and 100%. In another word, τ_n must be bigger than $\bar{\tau}_a$. A ε_a Lower than 50% represents the short-circuit flow and defection of the system in ventilation. In this scenario, the mean age of air at exhaust is smaller than the mean age of air of the entire area ($\tau_n < \bar{\tau}_a$).

4. Result and discussion

3.1. Temperature and contaminant distribution

Temperature contours have been depicted in Fig. 5. According to Fig. 5 and table 4, the hybrid scenarios had lower average temperature compared to the standalone DV system, and were able to maintain the recommended temperature range suggested by ASHRAE [31]. Moreover, the local thermal discomfort index was in a standard range for both occupants, whereas in the index was out of standard range in most cases of the DV system. Totally one can say that the hybrid DV-CC would result in an improved thermal sensation.

The contaminant distribution analysis was divided into three sections: 1. Contaminant distribution throughout the room 2. Contaminant concentration at the inhaled zone. 3. Ventilation effectiveness.

Fig. 6 determines the contaminant contours at the central plane (x = 2 m) for all of the cases. As shown in Fig. 6, the contaminant profile was completely stratified and ideal in the standalone modes of cases 1 and 2. Nevertheless, by addition of the chilled surface, inversion phenomenon divided the contaminant throughout the room and turned the profile close to a diluting base system. Therefore, it was obvious that the chilled ceiling caused disturb effect due to deteriorating the stratified form of the particles.

Based on Fig. 6, the transference of the contaminant had defection in the standalone modes of cases 3 and 4. Due to inefficient places of the exhaust vent in these two cases, the healthy and fresh air left the room without carrying any particles. Consequently, the polluted air remained above the occupants. However, in the hybrid mode of cases 2 and 3, the contaminant was relatively divided throughout the room. Unlike pervious cases, the mixing impact of the inversion phenomenon improved the contaminant distribution. Fig. 7 shows each case study's normalized CO2 concentration profile at the introduced poles (see Fig. 1). Regardless of the exhaust vent location, the contaminant concentration was higher in the lower heights of the room in the hybrid CC/DV system which was caused by the inversion phenomenon. The most important height for analysis is between 1 - 1.5 where the occupants breathing the air. According to Fig. 7, In cases 1 and 2, the CC/DV curve shows higher CO_2 concentration at the breathing zone in most of the poles. In case 1, The highest disturb effect in the breathing zone was occurred in pole 4 at 1.5 m height from the floor.

At this height, the contaminant concentration was 0.65 and 1.07 for the standalone and the hybrid mode, respectively. Based on Fig. 7 for case 2, the hybrid CC/DV system was unable to improve the efficient performance of LEV strategy. However, the disturb effect was relatively reduced compared to the first case at the breathing zone. improvement by the hybrid mode was achieved in cases 3

and 4. For instance, in case 3, the CO_2 concentration in the breathing zone was reduced from 1.45 to 1.07 by addition of the chilled ceiling in pole 2 at the height of 1 m from the floor. The highest improvement in case 4 was occurred in pole 2, as well. Where the CO_2 concentration was reduced from 1.35 to 1.00 at the height of 1.2 m from the floor. The improvement by the chilled ceiling was more obvious in case 3 compared to case 4. It means chilled surface was helpful in contaminant distribution when the exhaust vent was placed in less efficient places. However, there was no improvement when the exhaust vent was placed in the optimized place. In addition, despite the improvement which was achieved in cases 3 and 4, the hybrid performance in case 2 still suggested the safer environment compared to hybrid mode of cases 3 and 4 in most of the poles. Therefore, LEV was a better strategy rather than ceiling or low height exhaust strategy.

By analyzing the results of the contaminant concentration only at the inhaled zone, it was obtained that all of the hybrid cases had disturb effects compared to the standalone mode. Fig. 8 (a) and (b) determines the normalized CO_2 concentration at the inhaled zone for occupant 1 and 2, respectively. In case 1, the CO_2 concentration was increased from 0.80 to 0.97 for occupant 1 and the index increased from 0.48 to 0.88 for occupant 2 by addition of the chilled surface. In case 2, the CO_2 concentration was increased from 0.75 to 0.87 for occupant 1 and the ascending trend was obvious in occupant 2 which inversion phenomenon increased the index from 0.41 to 0.73. In case 3, the same trend was repeated and the concentration was increased from 1.05 to 1.17, and 0.88 to 0.97 for occupant 1 and 2, respectively. In the standalone mode of case 4, the index was 0.93 and 0.59 for occupant 1 and 2, respectively. As a result, the values in the hybrid mode passed from the allowable values for occupant 1 as CO_2 concentration raised until 1.08 and 0.91 for occupant 1 and 2, respectively. It was clear that the CO_2 concentration was relatively kept in the stratified form for both occupants in the hybrid mode of case 2. In another words, the normalized CO_2 concentration was lower than unity. It means LEV strategy was able to maintain the safe environment around the occupants' nose even by conjunction of DV and CC systems. All of the chilled ceiling effects on the contaminant distribution can be summarized in the ventilation effectiveness performance. According to Fig. 8 (c), case 3 had the lowest value compared to the other cases. However, addition of a chilled surface improved the index from 0.80 to 0.85. In case 4, the index for the standalone mode was equal to 1.00 and ventilation effectiveness had weaker performance in the hybrid mode which the value decreased to 0.93. Both hybrid modes of cases 3 and 4 had values less than unity which reported serious defection in transference of the particles to the outside environment in the presence of a chilled surface. Nevertheless, the value of the index was more than unity in cases 1 and 2 even by addition of a chilled surface. In case 2 the index was reduced from 1.46 to 1.22. It means, by usage of LEV method, it was possible to maintain the ventilation effectiveness of the system in the hybrid mode.

4.2. MAA and ACE analyze

Fig. 9 (a) and (b) determines the MAA index at the breathing zone for occupant 1 and 2, respectively. According to the results, addition of the chilled surface caused poorer MAA compared to the standalone mode. However, the disturb effect was vary according to the exhaust vent location. For instance, In the standalone mode of case 2, the MAA index were equal to 768 and 662 (s) for occupant 1 and 2, respectively. Addition of the chilled ceiling increased the values until 907 and 776 (s) for occupant 1 and 2, respectively. Similar increase was obvious in the other cases. Nevertheless, due to better performance of the system in cases 1 and 2, increase of the MAA index was less considerable than the hybrid mode of cases 3 and 4.

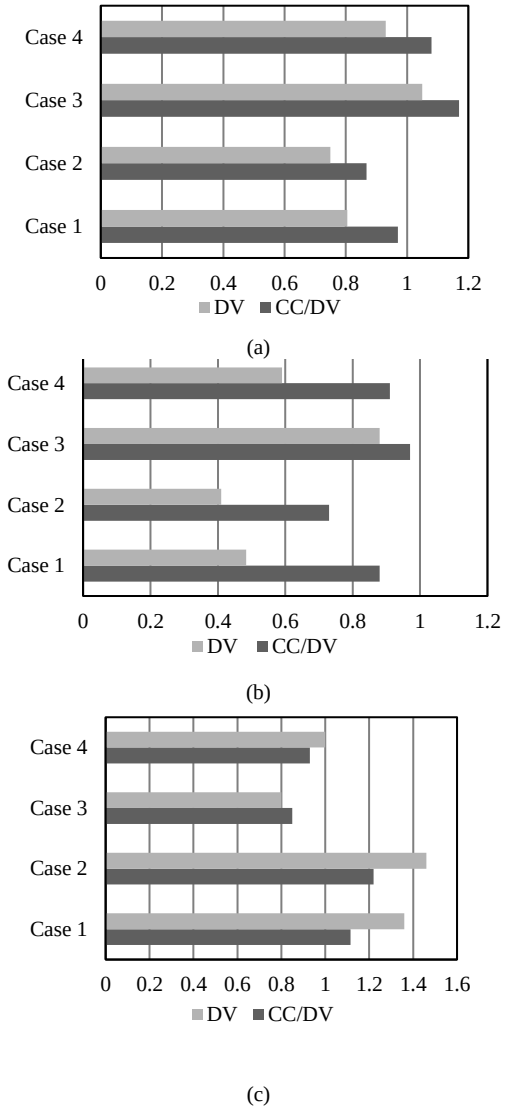

Fig. 8. (a) CO_2 concertation at the inhaled zone of occupant 1; (b) CO_2 concertation at the inhaled zone of occupant 2; (c) result of ventilation effectiveness

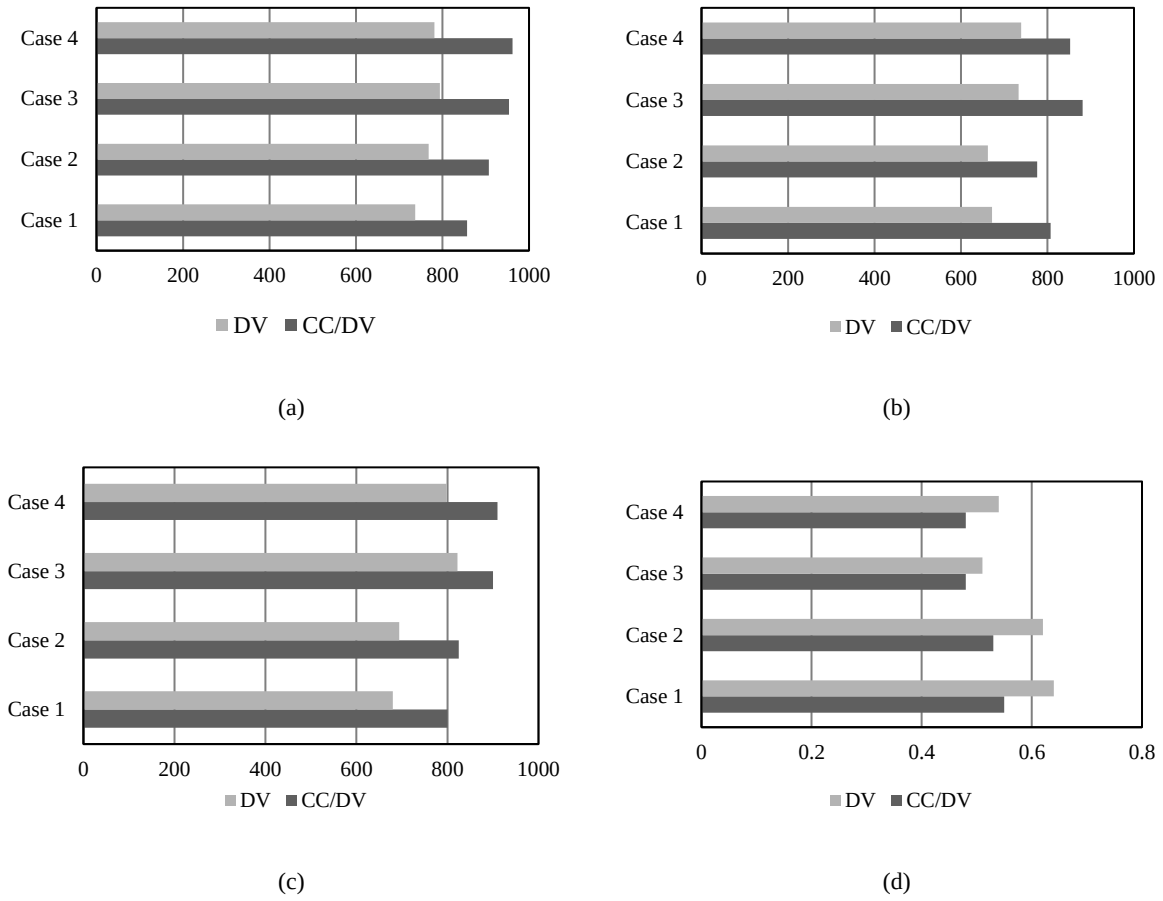

Fig. 9. the result of MAA (s) index along (a) Occupant 1; (b) Occupant 2; (c) Entire zone; (d) ACE index

Fig. 9 (c) represents the effects of the chilled ceiling on the MAA for the entire zone for each case study. The increase in the MAA index can be found in this figure, as well. For instance, the MAA of the entire zone was increased from 694 to 825 (s) by addition of the chilled surface in case 2. The similar result was obtained in case 1. Therefore, cases 1 and 2 had the lowest disturb effect compared to cases 3 and 4.

Fig. 9 (d) shows the results of ACE index. According to the results, addition of the chilled ceiling caused disturb effect regardless of the exhaust vent location. In both cases 3 and 4, the hybrid performance of CC and DV system caused defection in renewing the operating air due to unaccepted values of ACE index. Nevertheless, due to acceptable value of the ACE in the standalone performance of cases 1 and 2, the index was still in the allowable range even by conjunction of DV and CC systems.

Conclusion

Conclusion may review the main points of the author work. Also, it could include application of proposed method and suggestion for feature research.

In this study, the effects of a chilled ceiling on indoor air quality (IAQ) in a displacement ventilation (DV) system were investigated. In order to analyze, four places for exhaust vent were considered. The scenarios were included local exhaust vent (LEV), low height exhaust strategy, and two cases for the near ceiling exhaust vent. The important results are listed as below:

- The average temperature of the room was higher than suggested values of ASHRAE standard 55 in standalone DV system. However, CC/DV systems can offer a favorable thermal sensation for the occupants.
- The effects of the chilled ceiling on the contaminant distribution outside the micro-environment of the occupants were depended on the exhaust vent location. When the exhaust vent was placed at the low height of the room, the chilled ceiling positively affected the contaminant distribution. Nevertheless, in more optimized place (LEV strategy), addition of the chilled ceiling caused disturb effect, and there were no improvements.
- Based on the results, in the hybrid CC/DV systems, the normalized CO_2 concentration at the inhaled zones were increased between 11.4% to 83.3% according to the exhaust vent location. However, by the LEV

strategy it was possible to maintain the normalized CO_2 fraction less than unity (acceptable range) even by the mentioned increment of the concentration.

- The effects of the chilled ceiling on the ventilation effectiveness were also negetive. The deficiency was between 7% to 18% depending on the exhaust vent location. Neverthless, the LEV strategy was able to keep the index in the allowable range even by adding a chilled surface.
- Chilled surface caused poorer MAA at both breathing zone and the entire zone. The same result was observed for the ACE index.
- By LEV strategy, it was possible to maintain all of the IAQ requirements with a safe inhaled zone in the hybrid CC/DV system along with improved thermal sensation compared to the standalone DV mode.

Nomenclature

ρ	Density of air (kg/m^3)
P	Static pressure of air (Pa)
P_{op}	Operating pressure (Pa)
$\vec{v}$	Velocity (m/s)
$\vec{g}$	Gravitational acceleration (m/s^2)
$\bar{\bar{\tau}}$	Stress tensor (Pa)
R	Universal gas constant (J/K. mol)
M_w	Molecular weight of the gas
h	Sensible enthalpy (J)
c_p	Specific heat capacity at constant press (J/kg. K)
τ	Mean age of air (s)
τ_n	Nominal time constant (s)
$\bar{\tau}_a$	Room mean age of air (s)
Γ_t	Effective diffusion coefficient
ε_n	Normalized CO_2 concentration at a point
ε_e	Ventilation effectiveness
ε_a	Air change efficiency
C	CO_2 concentration at a point
C_s	CO_2 concentration at opening diffusers
C_e	CO_2 concentration at exhaust vent
C_p	CO_2 concentration at occupied zone
μ_t	Turbulent dynamic viscousity (Pa.s)
Sc_t	Turbulent Schmidt number
L	Distance from the nearest wall (m)
CC	Chilled ceiling
DV	Displacement Ventilation
STRAD	Stratified air distribution
UFAD	Under-floor air distribution
IAQ	Indoor air quality
LEV	Local exhaust vent

References

[1] M. S. Yeo, I. H. Yang, K.-W. Kim, Historical changes and recent energy saving potential of residential heating in Korea, Energy and Buildings 35(7) (2003) 715-727.

[2] B. W. Olesen, Radiant floor heating in theory and practice, ASHRAE Journal 44 (2002) 19-26.

[3] K. N. Rhee, K. W. Kim, A 50 year review of basic and applied research in radiant heating and cooling systems for the built environment, Building and Environment 91 (2015) 166-190.

[4] R. A. Memon, S. Chirarattananon, P. Vangtook, Thermal comfort assessment and application of radiant cooling: a case study, Building and Environment 43 (2008) 1185-1196.

[5] C. Wilkins, R. Kosonen, Cool ceiling system: a European air-conditioning alternative, ASHRAE Journal (1992) 34-41.

[6] M. Koschenz, V. Dorer, Interaction of an air system with concrete core conditioning, Energy and Building 30 (1999) 139-145.

[7] J. L. Niu, L. Z. Zhang, H .G. Zuo, Energy savings potential of chilled-ceiling combined with desiccant cooling in hot and humid climates, Energy and Building 34 (2002) 487-495.

[8] S. Wang, M. Morimoto, H. Soeda, T. Yamashita, Evaluating the low exergy of chilled water in a radiant cooling system, Energy and Building 40 (2008) 1856-1865.

[9] S. Schiavon, F. Bauman, B. Tully, J. Rimmer, Chilled ceiling and displacement ventilation system: laboratory study with high cooling load, Science and Technology for the Built Environment, 21 (2015) 944-956.

[10] A. Novoselac, J. Srebric, A critical review on the performance and design of combined cooled ceiling and displacement ventilation systems, Energy and Building 34 (2002) 497-509.

[11] F. Bauman, T. Webster, Outlook for underfloor air distribution, ASHRAE Journal 43 (6) (2001) 18-27.

[12] L. Zhou, F. Haghighat, Optimization of ventilation system design and operation in office environment, Part I: Methodology, Building and Environment, 44 (2009) 651-656.

[13] R. A. Memon, S. Chirarattananon, P. Vangtook, Thermal comfort assessment and application of radiant cooling: A case study, Building and Environment, 43 (7) (2008) 1185-1196.

[14] T. Catalina, J. Virgone, F. Kuznik, Evaluation of thermal comfort using combined CFD and experimentation study in a test room equipped with a cooling ceiling, Building and Environment, 44 (8) (2009) 1740-1750.

[15] J. Miriel, L. Serres, A. Trombe, Radiant Ceiling Panel Heating-Cooling Systems:

Experimental And Simulated Study of The Performances, Thermal Comfort And Energy Consumptions, Applied Thermal Engineering, 22 (16) (2002) 1861–1873.

[16] W. H. Chiang, C. Y. Wang, J. S. Huang, Evaluation of cooling ceiling and mechanical ventilation systems on thermal comfort using CFD study in an office for subtropical region, Building and Environment, 48 (2012) 113-127.

[17] S. Schiavon, F. Bauman, B. Tully, J. Rimmer, Chilled ceiling and displacement ventilation system: laboratory study with high cooling load, Science and Technology for the Built Environment 21 (2015) 944-956.

[18] D. L. Loveday, K. C. Parsons, A. H. Taki, S. G. Hodder, Displacement ventilation environments with chilled ceilings: thermal comfort design within the context of the BS EN IS07730 versus adaptive debate, Energy and Building 34 (6) (2002) 573-579.

[19] D. Loveday, K. Parsons, A. Taki, S. Hodder, L. Jeal, Designing for thermal comfort in combined chilled ceiling/displacement ventilation environments, ASHRAE Transactions 104 (1998).

[20] N. Ghaddar, K. Ghali, R. Saadeh, A. Keblawi, Design charts for combined chilled ceiling displacement ventilation system (1438-RP), ASHRAE Transactions 143 (2) (2008) 574–587.

[21] D. Xie, Y. Wang, H. Wang, S. Mo, M. Liao, Numerical analysis of temperature non-uniformity and cooling capacity for capillary ceiling radiant cooling panel, Renewable Energy 87 (2016) 1154-1161.

[22] B. Ning, Y. Chen, H. Liu, S. Zhang, Cooling capacity improvement for a radiant ceiling panel with uniform surface temperature distribution, Building and Environment 102 (2016) 64-72.

[23] M. Behne, Indoor air quality in rooms with cooled ceilings.: Mixing ventilation or rather displacement ventilation?, Energy and Buildings 30(2) (1999) 155-166.

[24] B. Rahmati, A. Heidarian, A.M. Jadidi, Investigation in performance of a hybrid under-floor air distribution with improved desk displacement ventilation system in a small office, Applied Thermal Engineering 138 (2018) 861-872.

[25] P. Raftery, K. H. Lee, T. Webster, F. Bauman, Performance analysis of an integrated UFAD and radiant hydronic slab system, Applied Energy, 90 (2012) 250-257

[26] Z. L. B. Yang , A.K. Melikov , A. Kabanshi , C. Zhang , F.S. Bauman , G. Cao , H. Awbi , H. Wig¨o , J. Niu , K.W.D. Cheong , K.W. Tham , M. Sandberg , P.V. Nielsen , R. Kosonen , R. Yao , S. Kato , S.C. Sekhar , S. Schiavon , T. Karimipanah , X. Li and Z. Lin, A review of advanced air distribution methods - theory, practice, limitations and solution , Energy and Buildings, 202 (2019).

[27] Z. Shi, Z. Lu, Q. Chen, Indoor airflow and contaminant transport in a room with coupled displacement ventilation and passive-chilled-beam systems, Building and Environment, 161 (2019).

[28] Q. Chen, W .Xu, A zero-equation turbulence model for indoor airflow simulation, Energy and Buildings, 28 (1998) 137-144.

[29] N. Kobayashi, Q. Chen, Floor-Supply Displacement Ventilation in a Small Office, Indoor and Built Environment, 12 (4) (2003) 281-291.

[30] ISO7730, Moderate Thermal Environments – Determination of the PMV and PPD Indices and Specification of the Conditions for Thermal Comfort, International Standard Organization, Geneva, (1994).

[31] ASHRAE Standard 55, Thermal Environmental Conditions for Human Occupancy, American Society of Heating, Refrigerating and Air-Conditioning Engineers, Inc., Atlanta, (2004).